Defining the Transmembrane Helix of M2 Protein from Influenza A by Molecular Dynamics Simulations in a Lipid Bilayer

Defining the Transmembrane Helix of M2 Protein from Influenza A by Molecular Dynamics Simulations in a Lipid Bilayer

Lucy R. Forrest,* D. Peter Tieleman,[#] and Mark S. P. Sansom*

*Laboratory of Molecular Biophysics, Department of Biochemistry, University of Oxford, Oxford OX1 3QU, England, and [#]BIOSON Research Institute and Department of Biophysical Chemistry, University of Groningen, 9747 AG Groningen, The Netherlands

ABSTRACT   Integral membrane proteins containing at least one transmembrane (TM) α-helix are believed to account for between 20% and 30% of most genomes. There are several algorithms that accurately predict the number and position of TM helices within a membrane protein sequence. However, these methods tend to disagree over the beginning and end residues of TM helices, posing problems for subsequent modeling and simulation studies. Molecular dynamics (MD) simulations in an explicit lipid and water environment are used to help define the TM helix of the M2 protein from influenza A virus. Based on a comparison of the results of five different secondary structure prediction algorithms, three different helix lengths (an 18mer, a 26mer, and a 34mer) were simulated. Each simulation system contained 127 POPC molecules plus $\sim$3500–4700 waters, giving a total of $\sim$18,000–21,000 atoms. Two simulations, each of 2 ns duration, were run for the 18mer and 26mer, and five separate simulations were run for the 34mer, using different starting models generated by restrained in vacuo MD simulations. The total simulation time amounted to 11 ns. Analysis of the time-dependent secondary structure of the TM segments was used to define the regions that adopted a stable α-helical conformation throughout the simulation. This analysis indicates a core TM region of $\sim$20 residues (from residue 22 to residue 43) that remained in an α-helical conformation. Analysis of atomic density profiles suggested that the 18mer helix revealed a local perturbation of the lipid bilayer. Polar side chains on either side of this region form relatively long-lived H-bonds to lipid headgroups and water molecules.

INTRODUCTION

Ion channels are formed in lipid bilayers by integral membrane proteins and enable selected ions to move rapidly ($\sim 10^7$ ions s^{-1} channel^{-1}) across membranes. Ion channels are important in numerous cellular processes, principally electrical signaling (Hille, 1992), but also in other functions such as facilitating the uncoating of viral genomes (Sansom et al., 1998a). To understand the physical events underlying the biological properties of channels, one must characterize their structures and their dynamic behavior. However, because ion channels are membrane proteins, we remain relatively ignorant of their three-dimensional structures. Indeed, at the time of writing a high-resolution crystallographic structure is known for only one ion channel, namely KcsA, a bacterial K$^+$ channel (Doyle et al., 1998). This reflects a more general problem for membrane proteins. Although integral membrane proteins are thought to comprise $\sim$20–30% of most genomes (Boyd et al., 1998; Wallin and von Heijne, 1998), high-resolution structures have been solved for only a small number of membrane proteins. Thus it is important to make progress in the prediction and modeling of membrane protein structure.

The majority of integral membrane proteins appear to be made up of bundles of transmembrane (TM) α-helices (Sansom and Kerr, 1995). A number of different algorithms have been developed (Cserzo et al., 1994; Jones et al., 1994; Persson and Argos, 1994; Rost et al., 1996; von Heijne, 1992) that predict the number and location of such TM helices within the sequence of a membrane protein with a high degree of accuracy. However, for subsequent modeling and simulation studies, it is important that the exact locations in the amino acid sequence of the beginning and end of a TM helix are predicted accurately. Comparison of the results of applying different secondary structure prediction algorithms to the same membrane protein sequence or family of sequences suggests that this is rarely the case, as the predictions are in disagreement, and in those cases where experimental structural data are available, they also disagree with structure-based assignments of the beginnings and ends of TM helices (Hong and Sansom, unpublished results). This is presumed to reflect the small number of high-resolution structures that can be used to train prediction algorithms and the inherent limitations of secondary structure prediction in general (Russell and Barton, 1993). Thus it is useful to look for additional methods to aid the definition of TM helices. Realistic simulations, by including some consideration of the physical chemistry of protein/lipid/water interactions, might be able to refine the accuracy of prediction of purely sequence-based approaches. Furthermore, such simulations may provide additional information on the nature of helix/bilayer interactions at the atomic level. This is important in the context of the two-stage model of membrane protein folding (Popot and Engelman,

1990), which proposes that TM helices are in themselves stable in a bilayer environment and subsequently pack together to form an intact helix bundle.

Molecular dynamics (MD) simulations of TM helices in lipid bilayers are still in their infancy (Belohorcova et al., 1997; Shen et al., 1997; Tieleman et al., 1999d; Woolf, 1997). Therefore, it is important to have a number of relatively simple systems upon which to test such simulations. One such system is provided by the M2 protein from influenza A. The M2 protein forms low pH-activated proton channels within the viral membrane. It is involved in two stages of viral replication and is essential for virus function. Electrophysiological studies have shown that M2 can be blocked by antiviral drugs such as amantadine (Chizhmakov et al., 1996; Wang et al., 1993). M2 is a small membrane protein consisting of 97 residues, with the TM segment located toward the N-terminus. Spectroscopic (CD and solid-state NMR) studies indicate that the TM segment of M2 is α-helical (Duff et al., 1992; Kovacs and Cross, 1997). The functional channel is formed by parallel homotetramers of TM helices (Sakaguchi et al., 1997). A synthetic 23-mer peptide containing the predicted TM segment of M2 has been shown to generate ion channels in lipid bilayers (Duff and Ashley, 1992), although the conductance of such channels is somewhat higher than that estimated from expressed intact protein (Chizhmakov et al., 1996). Thus channel activity seems to reside in the TM segment. Overall, M2 is a relatively simple membrane protein that lends itself to analysis by simulation, to complement a considerable body of experimental data (Sansom et al., 1998a). M2 is representative of a large proportion of membrane proteins that contain a single TM helix (Arkin et al., 1997).

Molecular modeling studies of the M2 protein have been carried out by two research groups (Pinto et al., 1997; Sansom et al., 1997), and comparisons of independently derived models have suggested that the system is suitable for investigation in more detail (Forrest et al., 1998). However, such studies model the M2 helix bundle in vacuo. Klein and colleagues (Zhong et al., 1998a,b) have performed MD simulations of a 23-mer M2 helix bundle in a membrane-mimetic environment (a solvated octane slab).

Both studies are an approximation of the true environment of the TM helix, i.e., a phospholipid bilayer with water molecules on either side (Sansom et al., 1998b). Recent improvements in computing power and in the efficiency of the molecular dynamics code have made it possible to perform large-scale atomistic simulations of protein/lipid/water systems (Belohorcova et al., 1997; Shen et al., 1997; Tieleman and Berendsen, 1998; Tieleman et al., 1999d; Woolf, 1997). In this paper, MD simulations in an explicit bilayer/water environment are used to predict regions of stable α-helicity in the M2 TM segment. This is achieved by a combination of analysis of time-dependent secondary structure and the H-bonding interactions of polar side chains with lipid and water. A preliminary account of some of these results has been published in abstract form (Forrest and Sansom, 1998).

MATERIALS AND METHODS

Secondary structure prediction

The TM prediction programs used were MEMSAT v1.7 (Jones et al., 1994; http://globin.bio.warwick.ac.uk/~jones/memsat.html), DAS v2 (Cserzo et al., 1994; http://www.biokemi.su.se/~server/DAS), TopPred2 (von Heijne, 1992; http://www.biokemi.su.se/~server/TopPred2), TMAP v1.4 (Persson and Argos, 1994; http://www.embl-heidelberg.de/tmap/tmap-info.html), and PHDhtm (Rost et al., 1996; http://www.embl-heidelberg.de/predictprotein). Depending on the requirements of each algorithm, predictions were carried out on either a single M2 sequence, corresponding to the Weybridge strain of the virus (see Fig. 1), or on multiple alignments of several M2 sequences.

Generation of M2 helix models

Models of M2 α-helices were generated by restrained in vacuo MD, using a simulated annealing (SA) protocol as previously described in (Kerr et al., 1994). Briefly, idealized α-helical templates were generated. These were used in a two-stage SA-MD method incorporating distance restraints to maintain an α-helical backbone conformation. Each run of this procedure yielded an ensemble of 25 structures from which single structures were selected as the starting point of extended MD simulations in a bilayer/water environment.
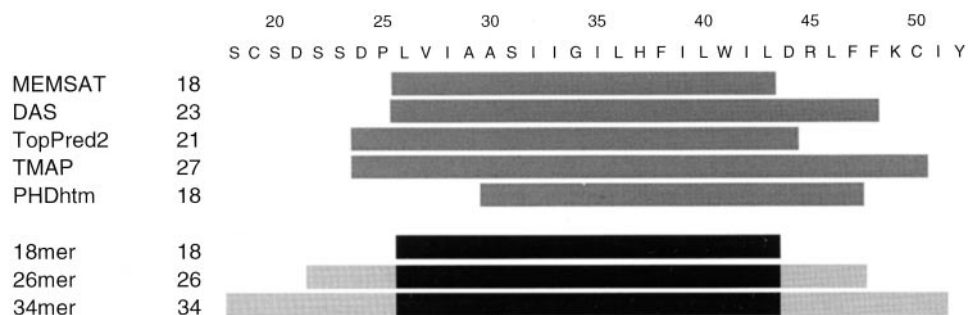

FIGURE 1   Defining TM segment of influenza A M2 protein. The amino acid sequence in the vicinity of the TM segment is shown at the top. The TM helix predictions of the various algorithms are shown as midgrey bars, with the numbers to the left of these indicating the number of residues. The definitions of the 18mer, 26mer, and 34mer TM helices used in the MD simulations are shown below, as a black bar for the core 18mer and as light gray bars for the extensions at either end of this.

Setup of helix/bilayer/water simulation systems

M2 helix models were embedded in a preequilibrated lipid bilayer consisting of 128 molecules of 1-palmitoyl-2-oleoyl-*sn*-glycerol-3-phosphatidylcholine (POPC). A hole was generated in the bilayer by a short MD simulation in which a radial force was applied to generate a cylindrical hole of radius 0.7 nm, into which the M2 helix was inserted. Unfavorable lipid-protein contact made necessary the removal of a single POPC molecule, giving a final total of 127 lipid molecules. We had some concerns that this might generate asymmetrical stress within the bilayer, but previous simulations of an alamethicin helix in a transmembrane orientation (Tieleman et al., 1999d), also with 127 POPC molecules, suggested that this was not a serious problem in terms of, e.g., destabilization of the secondary structure. The whole system was solvated with a minimum of 30 SPC waters per lipid and then energy minimized. In those simulations where counterions were included, Na^+ ions were added by replacing water molecules at positions corresponding to the lowest Coulombic energy of the ion. Each system was once more energy minimized. An example of one system is shown in Fig. 2 *A*.

MD simulations

MD simulations were carried out using periodic boundary and NPT conditions. A constant pressure of 1 bar was applied independently in all three directions, using a coupling constant of $\tau_P = 1.0$ ps (Berendsen et al., 1984), allowing the bilayer/protein area to adjust to an optimum value. Water, lipid, and peptide were coupled separately to a temperature bath at 300 K, using a coupling constant $\tau_T = 0.1$ ps. Long-range interactions were dealt with by using a twin-range cutoff: 1.0 nm for van der Waals interactions, and 1.8 nm for electrostatic interactions. The time step was 2 fs, with either LINCS (Hess et al., 1997) or SHAKE (Ryckaert et al., 1977) used to constrain bond lengths.

The SPC water model used (Berendsen et al., 1981) has been shown to behave well in simple lipid/water simulations (Tieleman and Berendsen, 1996). The lipid parameters used have been shown to give a good reproduction of experimental properties of a DPPC bilayer and have been used in previous MD studies (Berger et al., 1997; Marrink et al., 1998; Tieleman et al., 1999a,b,d).

Computational details

MD simulations were carried out on a 10-processor, 195-MHz R10000 Origin 2000 and on a 72-processor, 195-MHz R10000 Origin 2000 and took ~8 days per processor per 1-ns simulation. Simulations and analysis were carried out using the GROMACS (Berendsen et al., 1995) suite (http://rugmd0.chem.rug.nl/~gmx/gmx.html), with secondary structure analysis with the DSSP algorithm (Kabsch and Sander, 1983). Initial models were generated using Xplor (Brünger, 1992). Structures were examined using Quanta (Biosym/MSI) and Rasmol, and diagrams were drawn with MolScript (Kraulis, 1991).

RESULTS

TM helix predictions

To determine the possible extent of the M2 TM helix that should be considered, five TM prediction methods were employed. The results (see Fig. 1; we also ran a hidden Markov model method (Sonnhammer et al., 1998) that yielded the same results as MEMSAT) yield predicted TM helices ranging from 18 residues to 27 residues in length. There is some disagreement over the beginning and end residues of the TM helix. To explore this further, three TM helix models were built by SA-MD, ranging in length from
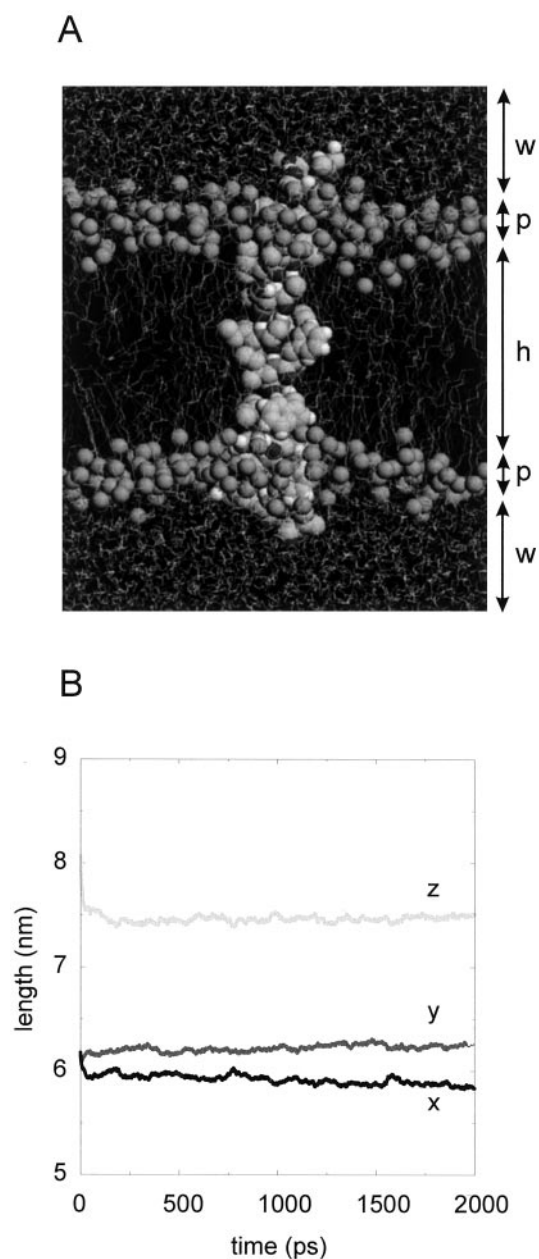

FIGURE 2 (*A*) Snapshot of the simulation system for 34merA. The peptide atoms and the carbonyl oxygens of the phospholipid molecules are shown in space-filling format. The approximate extents of the water (w), phospholipid headgroup (p), and hydrophobic core (h) regions of the system are indicated. (*B*) Periodic box dimensions as a function of time for the 18mer simulation.

18 to 34 residues (Fig. 1). The 18mer model was chosen to contain the core hydrophobic region predicted by most of the algorithms (with the exception of PHDhtm). It was the TM helix definition used in previous in vacuo modeling and simulation studies of M2 helix bundles (Sansom et al., 1997). The 26mer model contains the central 18mer, plus four residues (approximately one helix turn) added at each end. This model includes within it the TM helices predicted by MEMSAT, TopPred2, and PHDhtm, and all but one residue of that predicted by DAS. Finally, the 34mer model

TABLE 1   Simulation details

Simulation	Ionized residues	No. of Na$^+$ counterions	No. of waters	No. of atoms	Duration of simulation (ns)	Final Cα RMSD (nm)
18mer		0	3790	18153	2	0.18
26mer	D24,D44,R45	1	4712	21004	2	0.26
34merA	D21,D24,D44,R45	2	3803	18355	2	0.23
34merB	D21,D24,D44,R45,K49	1	3804	18359	2	0.23
34merC	D21,D24,D44,R45	2	3560	17626	1	0.18
34merD	D21,D24,D44,R45	2	4156	19414	1	0.22
34merE	D21,D24,D44,R45	2	4151	19399	1	0.13

consists of the 26mer plus a further turn of the helix at each end. The 34mer contains all residues of M2 predicted by any of the five algorithms to exist in the TM helix.

Progress of simulations

Details of the seven simulations are shown in Table 1. For the 18mer and 26mer, single 2-ns simulations were run. For the 34mer five simulations were run, each taking a different structure from the ensemble of 25 generated by SA-MD. These structures all had an α-helical backbone for all 34 residues, but differed in their side-chain conformations. Small differences in which residues were assumed to be ionized were made between the 34mer simulations, although these did not appear to have a significant effect. The drift of the TM helix structures from the initial starting models was assessed by examining the Cα RMSDs as a function of time (data not shown). In each case, after an initial rise over the first ~300 ps, the Cα RMSD reached a plateau for the remainder of the simulation. The final values of the Cα RMSD (see Table 1) range from 0.13 to 0.26 nm. Such values are typical for MD simulations of membrane proteins and peptides in a bilayer, even for those simulations starting with an x-ray structure (Tieleman and Berendsen, 1998), indicating that substantial conformational changes have not occurred.

To determine how any changes in lipid/protein packing might influence the periodic box size (given that a constant pressure algorithm was employed during these simulations), the box dimensions were monitored as a function of time for each simulation. The results (see Fig. 2 *B*) suggest some degree of relaxation in the plane of the bilayer from an initial ~6.2 × 6.2 nm^2 to ~5.8 × 6.3 nm^2, usually within the first 200 ps of the simulation. This is comparable to that seen in other simulations with this methodology (Tieleman et al., 1999a).

Examination of superimposed Cα traces for the simulations (Fig. 3) suggests that there is greatest conservation of structure in the relatively hydrophobic 18mer "core" of the TM helix, with greater structural variation at the extremities of the helix, as might be expected. This suggests that it is worth analyzing whether, e.g., changes in secondary structure occur during the course of the simulation.

Secondary structure

To determine which residues of M2 favor an α-helical conformation within a membrane environment, the peptide secondary structure has been analyzed as a function of time during the simulations. It is assumed that those residues which maintain α-helicity throughout a simulation prefer this conformation when located within the membrane.

Fig. 4 shows the secondary structure as a function of time for four simulations. The 18mer can be seen to remain α-helical throughout the simulation. In contrast, from ~650 ps on, the 26mer loses helicity in its C-terminal region (from Asp^{44} to Phe^{47}). Only two of the 34mers have been shown, as similar behavior is seen in the other three simulations. As with the 26mer, 34merA shows loss of helicity at the C-terminus (from Ile^{42} to Asp^{44}). The four N-terminal residues of 34merA lose α-helicity at ~750 ps. These patterns are reflected in the secondary structure analyses (not shown) of 34merC and 34merD. In contrast, both 34merB and 34merE show more limited loss of α-helicity in the region near residue 42, plus some loss of helicity at the N-terminus. These results indicate that there is some sensitivity of the
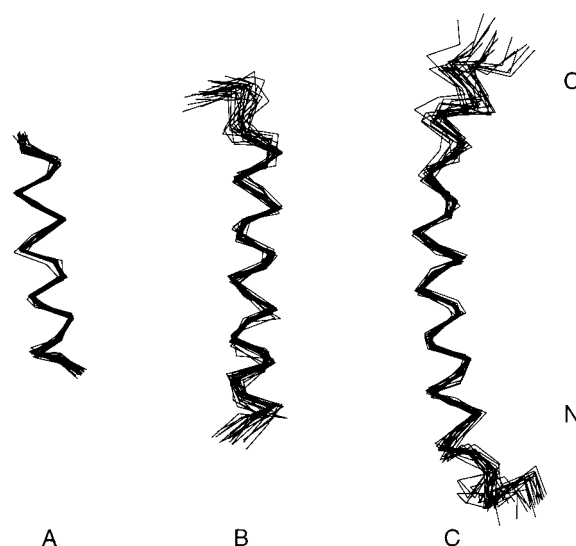

FIGURE 3   Superimposed Cα traces from the 18mer (*A*), 26mer (*B*), and 34merA (*C*) simulations. Each figure shows 20 structures, saved at 100-ps intervals. The structures are superimposed on their central 18 Cα atoms, with the C-termini of the helices uppermost.
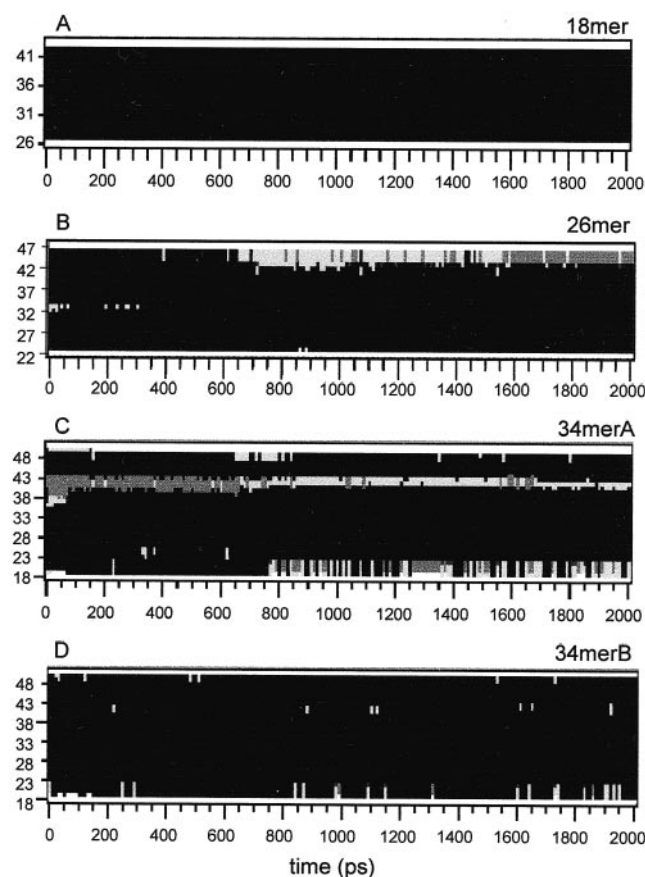
FIGURE 4 Secondary structural analysis (using DSSP; Kabsch and Sander, 1983) of the 18mer (*A*), 26mer (*B*), 34merA (*C*), and 34merB (*D*) simulations. Black squares represent α-helical residues, dark grey represents 3_{10}-helix, light gray represents a turn, and white squares represent random coil.

secondary structure behavior during the simulation to the exact initial structure and to the starting velocities of the atoms. However, the overall picture that emerges is that a region of M2 extending from residue ~22 to residue 43 is stable as an α-helix when simulated in a POPC bilayer.

One may probe the conformation of the TM segments in a little more detail by examining the backbone torsion angles. Plots of the φ and ψ angles of each residue averaged over the length of the simulation (Fig. 5) help to pinpoint those residues that deviate most markedly from α-helical conformation. For the 18mer (data not shown), as expected from the DSSP analysis, all backbone torsion angles remain close to their canonical α-helical values. The 26mer (Fig. 5 *A*) shows deviation from α-helicity at the N-terminus (residue 22) and close to its C-terminus (residues Trp[41], Leu[43], and Asp[44] in particular), confirming the DSSP indication of loss of α-helicity in that region. Detailed analysis of the (φ, ψ) values over time (not shown) for Leu[43], Asp[44], and Arg[45] indicates that these begin to deviate from α-helical values at ~700 ps, corresponding to the changes in secondary structure seen in Fig. 4. There is a marked increase in the Asp[44] φ angle at ~1550 ps.

Residues Trp[41] to Leu[43] also deviate from α-helical (φ, ψ) angles in the 34mer simulations, as do residues adjacent to them. In most of the five 34mer simulations, loss of α-helical conformations are observed in the region of the C-terminal residues Phe[47] to Ile[51], and in the N-terminal residues Ser[18] to Ser[22], with the effect being most dramatic at residue Ser[22]. On analysis of the (φ, ψ) angles over time, the Ser[22] ψ angle of 34merA does not change significantly until ~750 ps, corresponding to the secondary structure changes shown in Fig. 4. This behavior is mirrored in the DSSP and (φ, ψ) analysis of 34merD, e.g., Cys[19] deviates from an α-helical conformation at 100 ps, again matching changes in secondary structure seen in the DSSP plot (not shown).

It is interesting to note that the proline residue at position 25 remains in an α-helical conformation during all of the simulations. However, this proline does destabilize the preceding turn of α-helix, as might be expected given the distortions that proline residues have been observed to induce in α-helices (Barlow and Thornton, 1988). This is of interest in the context of a number of studies of prolines in TM helices (Brandl and Deber, 1986; Sansom, 1992; von Heijne, 1991; Woolfson et al., 1991).

Peptide/bilayer/water density profiles

In addition to the conformational dynamics of the M2 helix backbone, it is of interest to analyze the interactions of the helix with its bilayer and water environment. An overview of this may be obtained by examining the density profiles of water, lipid, and peptide atoms for the different simulations. Comparison of the profiles for the first and last 10 ps of each simulation revealed no significant changes, and so profiles averaged over the entire simulation period are shown in Fig. 6. For the 18mer, it is evident that the peptide density extends only to the extremities of the water density. Thus this rather short TM helix model is located entirely within the hydrophobic core of the bilayer. Furthermore, careful comparison of the lipid density profile for the 18mer (Fig. 6 *A*) with those for the 26mer and 34merA (Fig. 6, *B* and *C*) suggests that the shorter peptide may produce some reduction in the average bilayer thickness relative to the two longer peptides. However, most of the lipid molecules that contribute to this average thickness are relatively distant from the helix, thus obscuring possible effects of the peptide on the adjacent lipid. A more detailed analysis of the bilayer thickness around the protein (Tieleman et al., 1999c) revealed a considerable decrease in the immediate vicinity of the latter. For both the 26mer and, to a greater extent, the 34mer, the peptide atoms extend into the interfacial region, where lipid and water atoms are both present. However, even in the case of the 34mer, peptide does not extend beyond the extremities of the lipid density. Thus one should examine the simulations for evidence of interactions between the peptide side chains and the interfacial lipid/water environment.
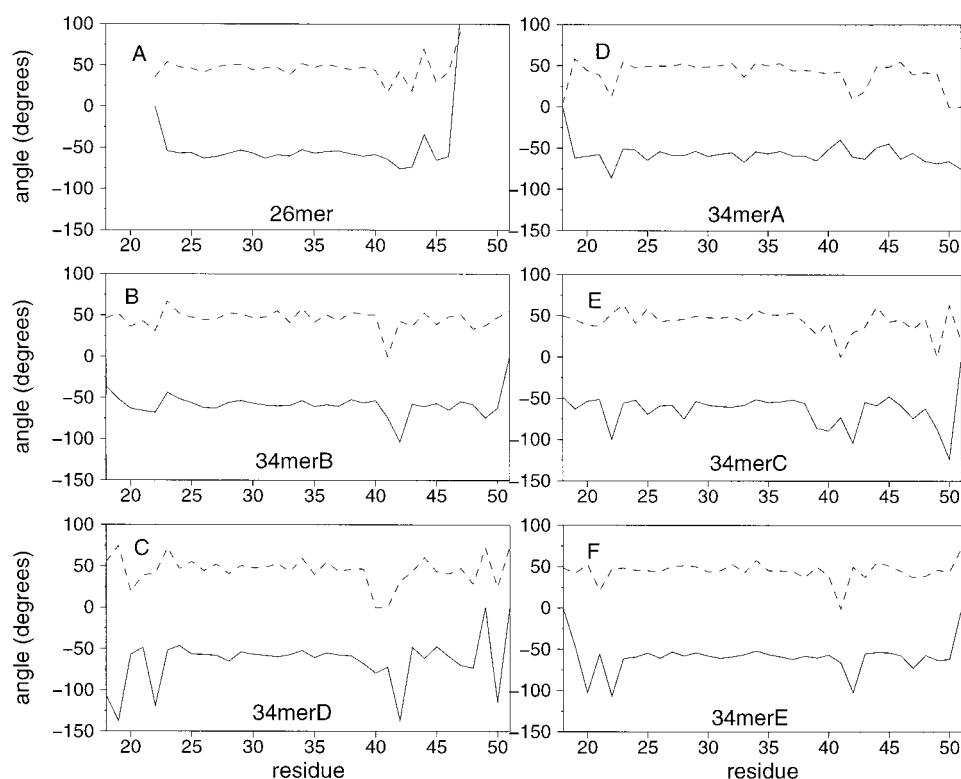
FIGURE 5 Average φ and ψ angles per residue for the 26mer (*A*), 34merA (*B*), 34merB (*C*), 34merC (*D*), 34merD (*E*), and 34merE (*F*) simulations. The φ values are shown using a solid line. The ψ angles (*broken line*) have been multiplied by -1 to represent φ and ψ on the same graph. For an ideal α-helix, $(\varphi, \psi) \approx (-57°, -47°)$.

Hydrogen bonds

Patterns of H-bond formation between the peptide and lipid or water have been analyzed. In considering the results of such analysis, it should be remembered that side-chain motions are relatively slow (Tieleman et al., 1999c) and H-bonds are long lasting, so side-chain interactions are incompletely sampled. The criteria used for assigning an H-bond were an H-donor-acceptor angle of $<60°$ and a donor-acceptor distance of <0.35 nm. Fig. 7 shows the fraction of time each residue spends forming a H-bond to either water or phospholipid. This fraction (f_H) was calculated as follows. If n_H is the total number of time steps during which a given residue is observed to form a H-bond, n_T is the total number of time steps in the simulation, and q is the number of observed types of H-bond formed by the residue in question during the simulation, then $f_H = n_H/(n_T \cdot q)$. Thus, if a given residue makes a single type of H-bond throughout the entire simulation, $f_H = 1$. If, for example, a serine hydroxyl donates an H-bond to two different lipid oxygens during the course of a simulation but always remains H-bonded to one or the other oxygen, $f_H = 0.5$.

The 18mer helix forms few H-bonds (data not shown), as would be anticipated from its location in the hydrophobic core of the bilayer. Residues Ile[26] to Ile[28] H-bond to water molecules with $f_H = 0.1$–0.2, and the Trp[41] residue H-bonds to a POPC molecule with a similar fraction. These interactions are all via backbone atoms.

In the 26mer (Fig. 7 *A*) H-bonding at the N-terminus is predominantly via the two serine residues. In particular, the side-chain hydroxyl of Ser[23] is H-bonded to water with a fraction of ~ 0.25. No H-bonding is observed for Trp[41], although some H-bonding to both lipid and water is seen at the C-terminus (residues Ile[42] through to Arg[45]). All of this H-bonding occurs from backbone atoms. On visual analysis, one can see that Asp[44] and Arg[45], whose side chains might be expected to H-bond the lipid and/or water, form H-bonds with one another, and the second NH donor of Arg[45] H-bonds to the backbone carbonyl of Trp[41]. The Asp[44]/Arg[45] interaction seems to correlate with loss of helicity in this region.

In the 34mers (Fig. 7, *B–F*), a more consistent pattern of H-bonding to POPC molecules is seen at the N-terminus than at the C-terminus, particularly at the serine residues 18, 20, 22, and 23. Analysis of individual contributions shows that in the 34merB and 34merD simulations, all of the serines have one H-bond that persists throughout the simulation, e.g., Ser[20] of 34merB H-bonds to O16 of POPC44 for a majority of the 2-ns simulation time (Fig. 8 *A*). The serine residues of 34merC and 34merE show a somewhat different behavior, with two or three H-bonds that make marked contributions, and the serine alternating between these, e.g., Ser[18] of 34merE H-bonds for equivalent amounts of time to oxygens 7, 16, and 33 of POPC47. The serines of 34merA demonstrate both of these types of behavior. Ser[18] and Ser[22] have one predominant H-bond each, whereas Ser[23] alternates equally between two H-bonding states to different lipids.

The interaction of Trp[41] with lipids is of interest, given the discussion of the possible role of Trp side chains in

FIGURE 6 Atomic density profiles along the bilayer normal for the 18mer (*A*), 26merA (*B*), and 34merA (*C*) simulations. In each case the profiles are shown for peptide (*bold lines*), lipid (*dotted lines*), and water (*broken lines*) atoms. The midplane of the bilayer is at $z = 0$ nm. (*D*) Density profiles as a function of time for the 34merA simulation. The four lines correspond to the density profile averaged over successive periods of 500 ps.
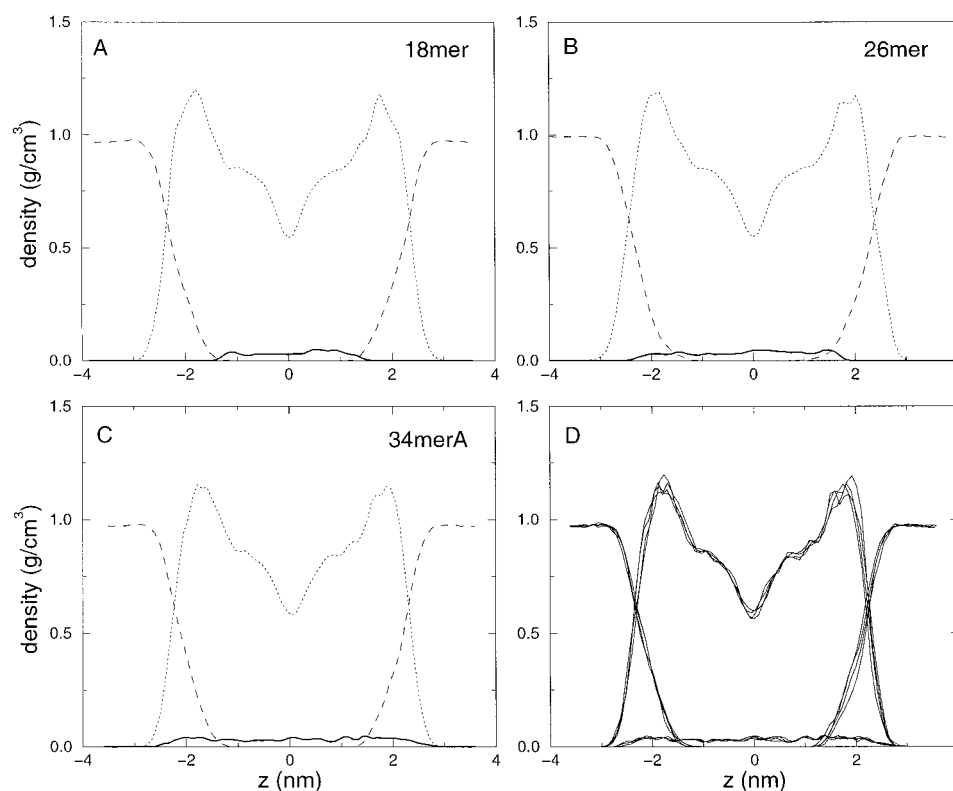
positioning membrane proteins within a bilayer (Grossfield and Woolf, 1998; Schiffer et al., 1992; Tieleman et al., 1999c; Weiss et al., 1991; Yau et al., 1998). 34merA and 34merB show considerable H-bonding interaction of Trp[41]

with lipid, but this is not seen for 34merC, 34merD, or 34merE. On more detailed investigation, the Trp[41] N-H of 34merB is seen to H-bond in a flickering manner to O14 of POPC60, although this only becomes apparent after ~700
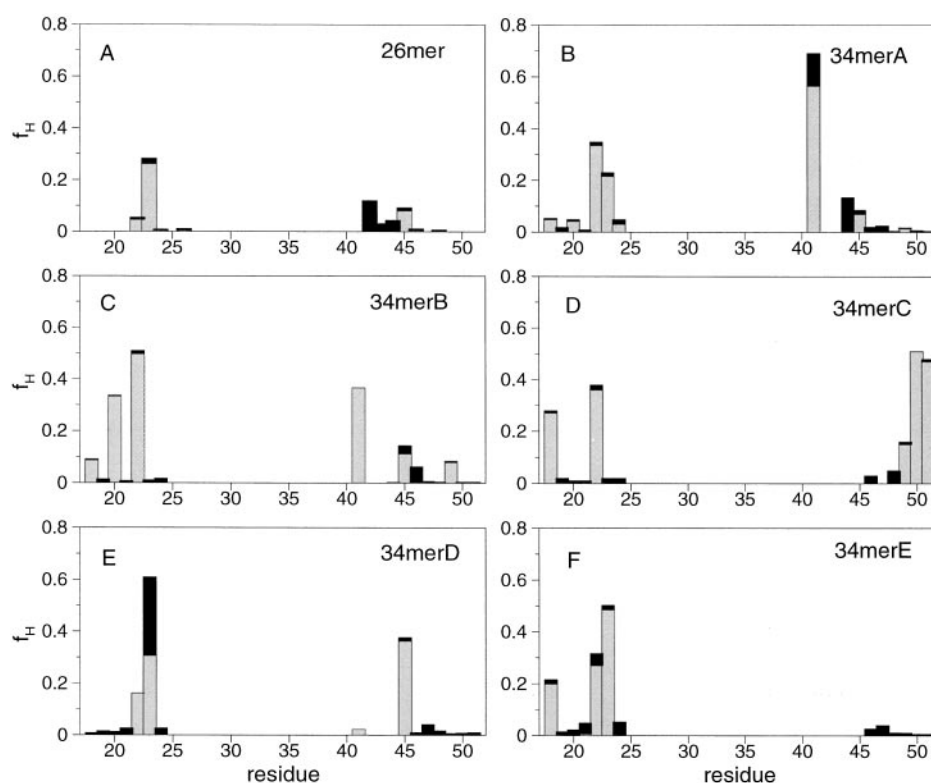

FIGURE 7 Fraction of H-bonding (f_H) (see text for definition) per residue for the 26mer (*A*), 34merA (*B*), 34merB (*C*), 34merC (*D*), 34merD (*E*), and 34merE (*F*) simulations. H-bonds to phospholipid are shown in pale gray, and H-bonds to water are shown in black.
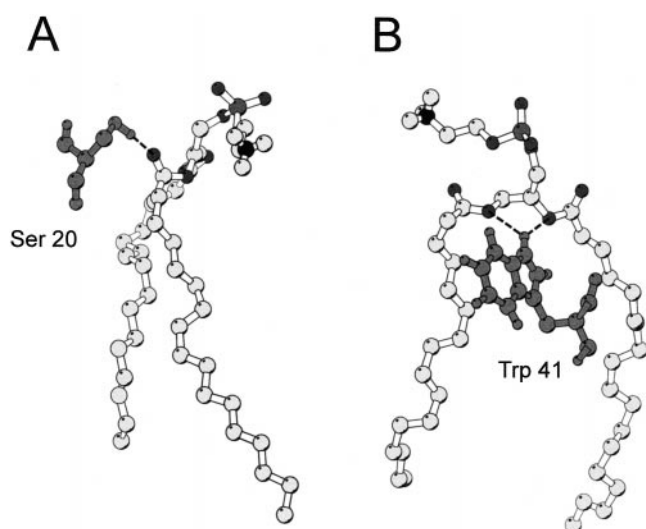
FIGURE 8 Snapshots of long-lasting H-bonds between polar side chains and lipid molecules. (*A*) From Ser[20] to O16 of POPC44, in simulation 34merB. (*B*) From Trp[41] to O14 and O33 of POPC60, in simulation 34merA. H-bonds are shown as broken lines.

ps. The Trp[41] N-H of 34merA shows two dominating H-bonds to oxygens 14 and 33 of POPC60 (Fig. 8 *B*).

Where suitable donors and acceptors are available, the contributions of the C-terminal residues Asp[44], Arg[45], and Lys[49] are seen to be coming from side-chain interactions rather than from the backbone. Note that although the f_H values may seem small, the large numbers of possible H-bonds (q) lower these numbers. For example, Arg[45] of 34merA shows 18 possible types of H-bonding, but one of them predominates, with a half-life of nearly 1 ns. This gives an overall fraction of less than 0.1.

Overall, it appears that there is no obvious correlation between the patterns of H-bonding and the stability/instability of α-helical conformation for residues in the interfacial region. However, it does seem that the H-bonds may be important for "locking" the protein into the lipid bilayer, although it is still rather difficult to arrive at an estimate of the relative contributions of H-bonding interactions in the interface and hydrophobic interactions in the bilayer core. The exact pattern of H-bonding fluctuates dynamically, as might be expected, given the fluctuating nature of the bilayer/water environment, although such fluctuations are relatively slow, resulting in incomplete sampling in nanosecond simulations.

DISCUSSION

Implications of results

The simulations presented above are, to the best of our knowledge, the first that use MD simulations in a full lipid bilayer and water environment to aid prediction of the TM helix of a membrane protein. Thus they extend the studies of Tobias et al. (1995) and of Nikiforovich (1998), who have used in vacuo calculations to aid TM helix prediction. Our

simulations are similar in spirit to those of Bodkin and Goodfellow (1995), Kovacs et al. (1995), Sessions et al. (1998), and Tieleman et al. (1999d), who have investigated peptide helix stability in membrane-mimetic solvents. A simulation-based approach extends and complements the many purely sequence-based prediction methods (Jones et al., 1994; Rost et al., 1996; Sonnhammer et al., 1998), which provide accurate predictions of the number and topology of TM helices, but relatively approximate locations for them within the sequence.

It should be noted that in these simulations we have assumed that the M2 helix adopts a transmembrane orientation, even though the pre- and post-TM polypeptide chain is not included. From a peptide perspective, this may represent a metastable system, although, e.g., He et al. (1996) and Huang and Wu (1991) have indicated some of the complexities of the surface/inserted equilibrium for membrane-active peptide helices. However, in the context of the two-state model of membrane protein folding (Popot and Engelman, 1990), isolated TM helices are thought to be a stable folding intermediate en route to an intact helix bundle.

It is of interest that in the current simulations the M2 helix does not show a pronounced tilt relative to the lipid bilayer normal. This is in contrast with, e.g., solid-state NMR data (Kovacs and Cross, 1997) and Fourier transform infrared data (Kukol et al., 1999). However, these latter studies are of the (presumed) tetramer of M2 and were conducted at relatively high peptide:lipid ratios, in contrast to the current study of an isolated TM helix. The difference suggests that helix tilt is a consequence of tetramer formation (Forrest et al., 1998) rather than of helix/bilayer interactions.

It is instructive to consider here the possible limitations of sequence-based methods of TM helix prediction and the refinements one might reasonably hope MD simulations could bring to such predictions. The main limitation of such predictions is probably that a dearth of high-resolution structural data for membrane proteins means that prediction methods have to be trained on topological (i.e., inherently low-resolution) data. It would be unreasonable to expect predictions to outperform the data on which they are trained, and indeed it is perhaps remarkable that these methods perform so well. Even when more high-resolution structures become available, it is likely that there will be a ceiling on their performance. As has been shown by, e.g., Russell and Barton (1993), multiple sequence alignment, which is used in most TM helix prediction methods, places an inherent limit on the accuracy of secondary structure predictions, regardless of the algorithm employed. What MD simulations may be able to add is a detailed consideration of the physicochemical interactions of the helix and the bilayer/water environment, particularly in the interfacial region. Although sequence-based predictions seem to be good at identifying the hydrophobic core of TM helices, and indeed this definition is used in the current simulations to determine the initial position of the model helix relative to the bilayer, MD simulations may be able to determine how far

a stable α-helical conformation projects beyond the bilayer core, where potential H-bonds to lipid and water compete with intrahelical H-bonds.

In the current study, we have assumed that the hydrophobic core of the TM helix, which is identified by sequence-based prediction methods, sits in the core of the bilayer. The question then arises, how far does the helix extend beyond the hydrophobic core? It is this aspect over which the sequence-based predictions appear to disagree and which we have tried to address via simulations. Thus MD simulations have been used to help determine the length of the TM helix of the M2 protein of influenza A. The overall conclusion from the various analyses of the trajectories is that a stable TM α-helix is formed by residues in the area of Ser[22] to Leu[43]. This considerably aids attempts to model and simulate the M2 helix bundle. This definition of the M2 TM helix is in closest agreement with the prediction from the TopPred2 algorithm (von Heijne, 1992). In contrast with our simulations, none of the sequence-based predictions included Ser[22] and Ser[23] at the N-terminus of the TM helix. At the C-terminus, the simulation results suggest that the TM helix ends at residue Leu[43]. This effect may be induced by ion pair formation by Asp[44] and Arg[45].

It should be noted that, in contrast to conventional wisdom for water-soluble proteins that serines are not favored in helices (Richardson and Richardson, 1989), our simulations indicate that Ser[22] and Ser[23] form an extension of the TM helix. However, serine-rich TM helices are found in synthetic channel-forming peptides (Åkerfeldt et al., 1993; Lear et al., 1988). They are also found in the pore-lining helices of the nicotinic acetylcholine receptor (Lester, 1992; Unwin, 1995) and in the M1, P, and M2 helices of the potassium channel KcsA (Doyle et al., 1998). Thus both experimental and simulation studies indicate that empirical rules for the secondary preference of amino acid types may not be simply transferred from water-soluble to membrane proteins (Deber and Goto, 1996). Serine side chains within a TM helix, if located in the hydrophobic core of the bilayer, may either satisfy their H-bonding requirements by interacting with the carbonyl oxygen of the preceding turn of the helix (Gray and Matthews, 1984), or, if in an interfacial location, may H-bond to, e.g., a phospholipid headgroup (see Fig. 8 *A*).

Analysis of H-bonding provides evidence for a role of polar side chains flanking the TM region in locking the helix within the membrane. MD simulations on a purely hydrophobic (Ala$_{32}$) helix chain in a DMPC bilayer (Shen et al., 1997) suggested that the need to form H-bonds to water in the aqueous and interfacial regions could lead to loss of α-helicity. Thus, although the introduction of polar or amphipathic aromatic residues may or may not directly stabilize an α-helical conformation, their capacity for hydrogen-bonding to the water and lipid headgroups in the interfacial environment may act to hold and stabilize the helix within the membrane environment. Simulations of the individual α-helices of bacteriorhodopsin in a 12-lipid DMPC bilayer (Woolf, 1997) support the suggestion that α-helices will be stabilized within a membrane if their residues can interact favorably with the interfacial region. Similarly, MD of the α-helical peptide ace-$K_2GL_{16}K_2A$-amide in a 12-lipid bilayer (Belohorcova et al., 1997) revealed that the lysine side chains maximized their interactions with water and were immobilized by H-bonding within the interfacial region. Again, this suggests that the effect of H-bonding is to hold the peptide in place. However, it should be remembered that these MD simulations still encompass a relatively small number of TM helix sequences, and further studies may be required before general rules emerge, particularly those concerning the relative contributions of H-bonding and hydrophobic interactions to TM helix/bilayer interactions.

Simulation protocol

There are several limitations to the simulation methods used in this paper. One concern is that the treatment of long-range electrostatic interactions with a cutoff may be too approximate. Pure bilayer simulations (Tieleman and Berendsen, 1996) using this method have produced reasonable agreement with experiment, but improved methods (e.g., Ewald summation) have been discussed (Tieleman et al., 1997; Tobias et al., 1997) and are becoming more feasible for large and complex systems. Other improvements would include increases in simulation time (Daura et al., 1998) and in the size of the lipid bilayer systems. Both of these increases would be necessary to incorporate possible large-scale fluctuations in bilayer structure.

The results reported here are sufficiently interesting to suggest the need for a detailed and systematic study of a number of factors that may influence the outcome of simulations of TM helices in a bilayer. In particular, these should attempt to address the effects of both static and dynamic helix/bilayer mismatch. By static mismatch we mean a difference in the length of the hydrophobic core of the TM helix and the equilibrium thickness of the hydrocarbon core of the bilayer. This could be investigated by simulations using different peptides and/or different lipids. By dynamic mismatch we mean the position along the bilayer normal of the center of the hydrophobic core of the TM helix relative to the center of the bilayer. Again, this could be probed by a further series of simulations. For example, in the current study we have assumed that the hydrophobic core of the TM helix should be aligned such that its center matches the center of the bilayer. This assumption could be tested by a series of simulations starting from successively displaced positions of the TM helix. Investigations of both of these approaches to mismatch are under way.

REFERENCES

Åkerfeldt, K. S., J. D. Lear, Z. R. Wasserman, L. A. Chung, and W. F. DeGrado. 1993. Synthetic peptides as models for ion channel proteins. *Acc. Chem. Res.* 26:191–197.

Arkin, I. T., A. T. Brünger, and D. M. Engelman. 1997. Are there dominant membrane protein families with a given number of helices? *Proteins Struct. Funct. Genet.* 28:465–466.

Barlow, D. J., and J. M. Thornton. 1988. Helix geometry in proteins. *J. Mol. Biol.* 201:601–619.

Belohorcova, K., J. H. Davis, T. B. Woolf, and B. Roux. 1997. Structure and dynamics of an amphiphilic peptide in a lipid bilayer: a molecular dynamics study. *Biophys. J.* 73:3039–3055.

Berendsen, H. J. C., J. P. M. Postma, W. F. van Gunsteren, A. DiNola, and J. R. Haak. 1984. Molecular dynamics with coupling to an external bath. *J. Chem. Phys.* 81:3684–3690.

Berendsen, H. J. C., J. P. M. Postma, W. F. van Gunsteren, and J. Hermans. 1981. Intermolecular Forces. Reidel, Dordrecht, the Netherlands.

Berendsen, H. J. C., D. van der Spoel, and R. van Drunen. 1995. GROMACS: a message-passing parallel molecular dynamics implementation. *Comp. Phys. Comm.* 95:43–56.

Berger, O., O. Edholm, and F. Jahnig. 1997. Molecular dynamics simulations of a fluid bilayer of dipalmitoylphosphatidycholine at full hydration, constant pressure and constant temperature. *Biophys. J.* 72:2002–2013.

Bodkin, M. J., and J. M. Goodfellow. 1995. Competing interactions contributing to alpha-helical stability in aqueous solution. *Protein Sci.* 4:603–612.

Boyd, D., C. Schierle, and J. Beckwith. 1998. How many membrane proteins are there? *Protein Sci.* 7:201–205.

Brandl, C. J., and C. M. Deber. 1986. Hypothesis about the function of membrane-buried proline residues in transport proteins. *Proc. Natl. Acad. Sci. USA.* 83:917–921.

Brünger, A. T. 1992. X-PLOR Version 3.1. A System for X-Ray Crystallography and NMR. Yale University Press, New Haven, CT.

Chizhmakov, I. V., F. M. Geraghty, D. C. Ogden, A. Hayhurst, M. Antoniou, and A. J. Hay. 1996. Selective proton permeability and pH regulation of the influenza virus M2 channel expressed in mouse erythroleukaemia cells. *J. Physiol. (Lond.).* 494:329–336.

Cserzo, M., J.-M. Bernassau, I. Simon, and B. Maigret. 1994. New alignment strategy for transmembrane proteins. *J. Mol. Biol.* 243:388–396.

Daura, X., B. Jaun, D. Seebach, W. F. van Gunsteren, and A. E. Mark. 1998. Reversible peptide folding in solution by molecular dynamics simulation. *J. Mol. Biol.* 280:925–932.

Deber, C. M., and N. K. Goto. 1996. Folding proteins into membranes. *Nature Struct. Biol.* 3:815–818.

Doyle, D. A., J. M. Cabral, R. A. Pfuetzner, A. Kuo, J. M. Gulbis, S. L. Cohen, B. T. Cahit, and R. MacKinnon. 1998. The structure of the potassium channel: molecular basis of K^+ conduction and selectivity. *Science.* 280:69–77.

Duff, K. C., and R. H. Ashley. 1992. The transmembrane domain of influenza A M2 protein forms amantadine-sensitive proton channels in planar lipid bilayers. *Virology.* 190:485–489.

Duff, K. C., S. M. Kelly, N. C. Price, and J. P. Bradshaw. 1992. The secondary structure of influenza A M2 transmembrane domain. *FEBS Lett.* 311:256–258.

Forrest, L. R., W. F. DeGrado, G. R. Dieckmann, and M. S. P. Sansom. 1998. Two models of the influenza A M2 channel domain: verification by comparison. *Folding Design.* 3:443–448.

Forrest, L. R., and M. S. P. Sansom. 1998. Simulations of the M2 channel for influenza A virus. *Biochem. Soc. Trans.* 26:S303.

Gray, T. M., and B. M. Matthews. 1984. Intrahelical hydrogen bonding of serine, threonine and cysteine residues within α-helices and its relevance to membrane-bound proteins. *J. Mol. Biol.* 175:75–81.

Grossfield, A., and T. B. Woolf. 1998. Aromatics at interfaces: molecular dynamics calculations of indoles in POPC bilayers. *Biophys. J.* 74:A303.

He, K., S. J. Ludtke, W. T. Heller, and H. W. Huang. 1996. Mechanism of alamethicin insertion into lipid bilayers. *Biophys. J.* 71:2669–2679.

Hess, B., H. Bekker, B. H. J. C., and F. J. G. E. M.B. H. J. C.F. J. G. E. 1997. LINCS: a linear constraint solver for molecular simulations. *J. Comp. Chem.* 18:1463–1472.

Hille, B. 1992. Ionic Channels of Excitable Membranes, 2nd Ed. Sinauer Associates, Sunderland, MA.

Huang, H. W., and Y. Wu. 1991. Lipid-alamethicin interactions influence alamethicin orientation. *Biophys. J.* 60:1079–1087.

Jones, D. T., W. R. Taylor, and J. M. Thornton. 1994. A model recognition approach to the prediction of all-helical membrane protein structure and topology. *Biochemistry.* 33:3038–3049.

Kabsch, W., and C. Sander. 1983. Dictionary of protein secondary structure: pattern recognition of hydrogen-bonded and geometrical features. *Biopolymers.* 22:2577–2637.

Kerr, I. D., R. Sankararamakrishnan, O. S. Smart, and M. S. P. Sansom. 1994. Parallel helix bundles and ion channels: molecular modelling via simulated annealing and restrained molecular dynamics. *Biophys. J.* 67:1501–1515.

Kovacs, F. A., and T. A. Cross. 1997. Transmembrane four-helix bundle of influenza A M2 protein channel: structural implications from helix tilt and orientation. *Biophys. J.* 73:2511–2517.

Kovacs, H., A. E. Mark, J. Johansson, and W. F. van Gunsteren. 1995. The effect of environment on the stability of an integral membrane helix: molecular dynamics simulations of surfactant protein C in chloroform, methanol and water. *J. Mol. Biol.* 247:808–822.

Kraulis, P. J. 1991. MOLSCRIPT: a program to produce both detailed and schematic plots of protein structures. *J. Appl. Crystallogr.* 24:946–950.

Kukol, A., P. D. Adams, L. M. Rice, A. T. Brünger, and I. T. Arkin. 1999. Experimentally based orientational refinement of membrane protein models: a structure for the influenza A M2 H^+ channel. *J. Mol. Biol.* (in press).

Lear, J. D., Z. R. Wasserman, and W. F. DeGrado. 1988. Synthetic amphiphilic peptide models for protein ion channels. *Science.* 240:1177–1181.

Lester, H. 1992. The permeation pathway of neurotransmitter-gated ion channels. *Annu. Rev. Biophys. Biomol. Struct.* 21:267–292.

Marrink, S. J., O. Berger, D. P. Tieleman, and F. Jahnig. 1998. Adhesion forces of lipids in a phospholipid membrane studied by molecular dynamics simulations. *Biophys. J.* 74:931–943.

Nikiforovich, G. V. 1998. A novel, non-statistical method for predicting breaks in transmembrane helices. *Protein Eng.* 11:279–283.

Persson, B., and P. Argos. 1994. Prediction of transmembrane segments utilising multiple sequence alignments. *J. Mol. Biol.* 237:182–192.

Pinto, L. H., G. R. Dieckmann, C. S. Gandhi, C. G. Papworth, J. Braman, M. A. Shaughnessy, J. D. Lear, R. A. Lamb, and W. F. DeGrado. 1997. A functionally defined model for the M_2 proton channel of influenza A virus suggest a mechanism for its ion selectivity. *Proc. Natl. Acad. Sci. USA.* 94:11301–11306.

Popot, J. L., and D. M. Engelman. 1990. Membrane protein folding and oligomerization: the two-state model. *Biochemistry.* 29:4031–4037.

Richardson, J. S., and D. C. Richardson. 1989. Principles and patterns of protein conformation. *In* Prediction of Protein Structure and the Principles of Protein Conformation. Plenum, New York. 1–98.

Rost, B., P. Fariselli, and R. Casadio. 1996. Topology prediction for helical transmembrane proteins at 86% accuracy. *Protein Sci.* 5:1704–1718.

Russell, R. B., and G. K. Barton. 1993. The limits of protein secondary structure prediction accuracy from multiple sequence alignment. *J. Mol. Biol.* 234:951–957.

Ryckaert, J. P., G. Ciccotti, and H. J. C. Berendsen. 1977. Numerical integration of the Cartesian equations of motion of a system with constraints: molecular dynamics of *n*-alkanes. *J. Comput. Phys.* 23:327.

Sakaguchi, T., Q. A. Tu, L. H. Pinto, and R. A. Lamb. 1997. The active oligomeric state of the minimalistic influenza virus M_2 ion channel is a tetramer. *Proc. Natl. Acad. Sci. USA.* 94:5000–5005.

Sansom, M. S. P. 1992. Proline residues in transmembrane helices of channel and transport proteins: a molecular modelling study. *Protein Eng.* 5:53–60.

Sansom, M. S. P., L. R. Forrest, and R. Bull. 1998a. Viral ion channels: molecular modelling and simulation. *Bioessays.* (in press).

Sansom, M. S. P., and I. D. Kerr. 1995. Principles of Membrane Protein Structure. *In* Biomembranes. JAI Press, London. 29–70.

Sansom, M. S. P., I. D. Kerr, G. R. Smith, and H. S. Son. 1997. The influenza A virus M2 channel: a molecular modelling and simulation study. *Virology.* 233:163–173.

Sansom, M. S. P., D. P. T. Tieleman, L. R. Forrest, and H. J. C. Berendsen. 1998b. Molecular dynamics simulations of membranes with embedded proteins and peptides: porin, alamethicin and influenza M2. *Biochem. Soc. Trans.* 26:438–443.

Schiffer, M., C. H. Chang, and F. J. Stevens. 1992. The functions of tryptophan residues in membrane proteins. *Protein Eng.* 5:213–214.

Sessions, R. B., N. Gibbs, and C. E. Dempsey. 1998. Hydogen bonding in helical polypeptides from molecular dynamics simulations and amide exchange analysis: alamethicin and melittin in methanol. *Biophys. J.* 74:138–152.

Shen, L., D. Bassolino, and T. Stouch. 1997. Transmembrane helix structure, dynamics, and interactions: multi-nanosecond molecular dynamics simulations. *Biophys. J.* 73:3–20.

Sonnhammer, E. L. L., G. von Heijne, and A. Krogh. 1998. A hidden Markov model for predicting transmembrane helices in protein sequences. *In* Proceedings of ISMB-98. AAAI Press.

Tieleman, D. P., and H. J. C. Berendsen. 1996. Molecular dynamics simulations of a fully hydrated dipalmitoylphosphatidycholine bilayer with different macroscopic boundary conditions and parameters. *J. Chem. Phys.* 105:4871–4880.

Tieleman, D. P., and H. J. C. Berendsen. 1998. A molecular dynamics study of the pores formed by *E. coli* OmpF porin in a fully hydrated POPE bilayer. *Biophys. J.* 74:2786–2801.

Tieleman, D. P., H. J. C. Berendsen, and M. S. P. Sansom. 1999a. An alamethicin channel in a lipid bilayer: molecular dynamics simulations. *Biophys. J.* 76:1757–1769.

Tieleman, D. P., J. Breed, H. J. C. Berendsen, and M. S. P. Sansom. 1999b. Alamethicin channels in a membrane: molecular dynamics simulations. *Faraday Discuss.* (in press).

Tieleman, D. P., L. R. Forrest, H. J. C. Berendsen, and M. S. P. Sansom. 1999c. Lipid properties and the orientation of aromatic residues in OmpF, influenza M2 and alamethicin systems: molecular dynamics simulations. *Biochemistry.* 37:17554–17561.

Tieleman, D. P., S. J. Marrink, and H. J. C. Berendsen. 1997. A computer perspective of membranes: molecular dynamics studies of lipid bilayer systems. *Biochim. Biophys. Acta.* 1331:235–270.

Tieleman, D. P., M. S. P. Sansom, and H. J. C. Berendsen. 1999d. Alamethicin helices in a bilayer and in solution: molecular dynamics simulations. *Biophys. J.* 76:40–49.

Tobias, D. J., J. Gesell, M. L. Klein, and S. J. Opella. 1995. A simple protocol for identification of helical and mobile residues in membrane proteins. *J. Mol. Biol.* 253:391–395.

Tobias, D. J., K. C. Tu, and M. L. Klein. 1997. Atomic-scale molecular dynamics simulations of lipid membranes. *Curr. Opin. Colloid Interface Sci.* 2:15–26.

Unwin, N. 1995. Acetylcholine receptor channel imaged in the open state. *Nature.* 373:37–43.

von Heijne, G. 1991. Proline kinks in transmembrane a-helices. *J. Mol. Biol.* 218:499–503.

von Heijne, G. V. 1992. Membrane protein structure prediction. Hydrophobicity analysis and the positive inside rule. *J. Mol. Biol.* 225:487–494.

Wallin, E., and G. von Heijne. 1998. Genome-wide analysis of integral membrane proteins from eubacterial, archean, and eukaryotic organisms. *Protein Sci.* 7:1029–1038.

Wang, C., K. Takeuchi, L. H. Pinto, and R. A. Lamb. 1993. Ion channel activity of influenza A virus M_2 protein: characterization of the amantadine block. *J. Virol.* 67:5585–5594.

Weiss, M. S., U. Abele, Weckesser, J., W. Welte, E. Schiltz, and G. E. Schulz. 1991. Molecular architecture and electrostatic properties of a bacterial porin. *Science.* 254:1627–1630.

Woolf, T. B. 1997. Molecular dynamics of individual α-helices of bacteriorhodopsin in dimyristoyl phosphatidylcholine. I. Structure and dynamics. *Biophys. J.* 73:2376–2392.

Woolfson, D. N., R. J. Mortishire-Smith, and D. H. Williams. 1991. Conserved positioning of proline residues in membrane-spanning helices of ion-channel proteins. *Biochem. Biophys. Res. Commun.* 175:733–737.

Yau, W. M., P. J. Steinbach, W. C. Wimley, S. H. White, and K. Gawrisch. 1998. Indole and N-methyl indole orientation in lipid bilayers. *Biophys. J.* 74:A303.

Zhong, Q., T. Husslein, P. B. Moore, D. M. Newns, P. Pattnaik, and M. L. Klein. 1998a. The M2 channel of influenza A virus: a molecular dynamics study. *FEBS Lett.* 434:265–271.

Zhong, Q. F., T. Husslein, D. M. Newns, P. Pattnaik, and M. L. Klein. 1998b. Influenza A M2 channel: a molecular dynamics study. *Biophys. J.* 74:A233.